UDC 004.891.3

L.S. Fainzilberg

GENERALIZED APPROACH TO BUILDING COMPUTER'S TOOLS OF PREVENTIVE MEDICINE FOR HOME USING

Ключові слова: превентивна медицина, інтелектуальні методи оброблення фізіологічних сигналів, смартфон.

Keywords: preventive medicine, intelligent methods, processing of biomedical signals, smartphone.

Introduction

The main goal of preventive medicine is to preserve human health through early detection and timely correction of imbalances in the body which may lead to the development of various diseases and their complications. To solve this important problem not only medical devices for clinical use are needed but also personalized devices can control the current state of the body at home.

Therefore it is no coincidence that the market for medical devices has significantly changed its direction from complex systems for clinic having recently relative stagnation to portable digital devices for independent use [1].

The development of such tools requires the use of intelligent information technologies (IT) which unlike traditional ones operate with generalized concepts — patterns. Such patterns provide more complete information about the functional systems of the body, and the analysis of such images forms a holistic picture of the phenomena under study.

The implementation of intelligent IT in medical means ensures adaptation to the individual characteristics of the organism of a particular user which makes it possible to carry out a personalized diagnosis of his functional state and to increase the reliability of assessing the risk of developing pathologies [2].

The purpose of the article is to develop a universal approach to the construction of personalized means of preventive medicine and, using examples of solving urgent applied problems, to demonstrate its effectiveness.

Conceptual idea of the proposed approach

In traditional medicine, diagnostic solutions are based on the concept of a medical norm [3]. The medical norm is usually reduced to the reference intervals of physiological indicators, which are determined on the basis of population trials of representative groups of practically healthy people.

However, clinical practice shows that in many people the course of diseases goes beyond the generally accepted framework, which leads to false positive and false nega-

tive diagnostic results. This is largely due to the fact that, in accordance with the existing standards [4], the values obtained in only 95 % of the surveyed group are used to determine the reference intervals.

It follows that the indicators of 5 % of healthy people (every twentieth), generally speaking, may not «fall» within the established framework of the reference interval. In other words, making diagnostic decisions according to the rule

$$\begin{aligned} &\text{Norm,} \quad \text{if } x_t \in X_0, \\ &\text{Attention, if } x_t \notin X_0, \end{aligned} \tag{1}$$

based on the analysis of the compliance of the current measurement result x_t with the medical norm X_0, may lead to erroneous results.

In addition, it is known that most physiological parameters are subject to significant spontaneous fluctuations (true biological variability) and this is considered a physiological norm [5–8]. Therefore, the episodic contact of a patient with a doctor, even when using the most advanced diagnostic system, can lead to an incorrect assessment of the risk of developing a disease if decisions are made only according to the rule (1).

Let us consider a different approach to making diagnostic decisions, which is based on the main principle of personalized medicine [9, 10] — to treat a patient, not a disease, taking into account the individual characteristics of the organism.

Let us assume that the patient has the ability to assess independently physiological parameters that carry information about the current state of the body over a sufficiently long period of time. The results of such observations form a set (training sample)

$$X = \{x_1, \ldots, x_N\}, \tag{2}$$

elements of which can have various shapes.

In some cases, it is a scalar value, for example, the glucose content in the blood. In other cases, it is a vector, the components of which are the values of a set of diagnostic indicators, for example, indicators of heart rate variability. Finally, the test result can have a more complex form, for example, the form of a phonospirogram characterizing the spectral components of the patient's respiratory noise.

We will assume that, regardless of the form of presentation of the results, for any two elements $x_i \in X$ and $x_j \in X$ it is possible to calculate a quantity $S(x_i, x_j)$ with the properties of a metric:

- $S(x_i, x_j) \geq 0$, and $S(x_i, x_j) = 0$ if and only if $x_i = x_j$;
- $S(x_i, x_j) = S(x_j, x_i)$;
- $S(x_i, x_j) \leq S(x_i, x_z) + + S(x_z, x_j)$, where $x_z \in X$.

The value $S(x_i, x_j)$ characterizes the proximity x_i and x_j in the metric space, in which we will make personalized decisions. To do this, we form a square matrix of distances $S(x_i, x_j)$, $i = 1, \ldots, N$, $j = 1, \ldots, N$, between all pairs of elements of the set (2):

$$R^{(N)} = \begin{pmatrix} S_{11}, & S_{12}, & \ldots, & S_{1N} \\ S_{21}, & S_{22}, & \ldots, & S_{2N} \\ & & \ldots & \\ S_{N1}, & S_{N2}, & \ldots, & S_{NN} \end{pmatrix}.$$

The matrix $R^{(N)}$ allows you to determine two integral values: the reference result $x_0 \in X$, which is the closest to all other observations of the training sample (2)

$$x_0 = \arg\min_{1 \le j \le N} \sum_{i=1}^{N} S_{ij}, \tag{3}$$

and the average deviation $\bar{S}$ of the results, which determines the ratio

$$\bar{S} = \frac{1}{N^2 - N} \sum_{i=1}^{N} \sum_{j=1}^{N} S_{ij}. \tag{4}$$

Condition (3) differs from the condition that is satisfied by the geometric center

$$\tilde{x}_0 = \arg\min_{x \in R^N} \sum_{i=1}^{N} S(x_n, x), \tag{5}$$

representing a point $\tilde{x}_0$ in N — dimensional space, from which the sum of the Euclidean distances to all points is minimal. Despite the external similarity (3) and (5), the values x_0 and $\tilde{x}_0$ are different: in the general case, the value $\tilde{x}_0$ may not coincide with any of the results of the training sample X, while $x_0 \in X$ it is the most characteristic result from the available observations.

This greatly simplifies the procedure for determining the reference result x_0 in comparison with the optimization procedure (5) for calculating the geometric center $\tilde{x}_0$, the practical implementation of which causes known computational difficulties [11].

Note that if the observations $x_1, \ldots, x_N$, are scalar values, then the procedure for determining the reference result x_0 becomes even easier: it is enough to calculate the median in a one-dimensional sample of cases $x_1, \ldots, x_N$. If, moreover $x_1, \ldots, x_N$, they are distributed symmetrically with respect to the mode (for example, according to the normal law), then the value c x_0 estimated by the arithmetic mean of the values $x_1, \ldots, x_N$.

For this, it is convenient to use the recurrence relation

$$x_0^{(n)} = x_0^{(n-1)} + \frac{1}{n}[x_n - x_0^{(n-1)}], \quad n = 1, 2, \ldots, \tag{6}$$

under the initial condition $x_0^{(0)} = 0$, which allows you to refine constantly the reference result x_0 as data accumulates, without saving the entire array of observations

$x_1,..., x_N$. In a similar way, you can calculate a value $\bar{S}$ that, as well as x_0 tends to a stable value with an increase in the number of observations in the training set X.

In cases where each of the results $x_n = (x_{n1}, x_{n2},..., x_{nM}) \in X$, $n = 1,..., N$ of the training set is a vector (an ordered set of M diagnostic features), the individual standard x_0 can be defined as a M-dimensional vector , $x_0 = (x_{01}, x_{02},..., x_{0M})$ the components of which are the medians or the average values of the corresponding components of the vectors from the training set. Note that in this case the reference vector x_0 does not necessarily belong to the set X.

Integral values x_0 and $\bar{S}$ characterize the individual characteristics of the organism of a particular patient: the standard x_0 reflects the central tendency of the observation results $x_1,..., x_N$, and the value $\bar{S}$ reflects the degree of variability of these observations.

Such information allows, in addition to (1), to make a personalized decision about the current state of the patient according to the rule:

$$\begin{aligned} &\text{Personal norm, if } S(x_t, x_0) \le \lambda\bar{S}, \\ &\text{Attentional, if } S(x_t, x_0) > \lambda\bar{S}, \end{aligned} \tag{7}$$

where x_t is the result of current observation and $\lambda \ge 1$ is the coefficient that provides the desired compromise between the sensitivity and specificity of the decisions made.

In addition, the analysis of belonging x_0 to the population norm X_0 makes it possible to assess the risk of the possible development of pathology according to the rule

$$\begin{aligned} &\text{Low risk, if } x_0 \in X_0, \\ &\text{High risk, if } x_0 \notin X_0, \end{aligned} \tag{8}$$

which is fundamentally different from rule (1), since the decision is made not according to the current observation x_t, but according to the perdonal standard x_0 calculated from the set of observations.

Thus, the proposed approach, in contrast to the traditional one, ensures the adaptation of diagnostic rules to the individual characteristics of the organism of a particular user, which increases the reliability of the decisions made.

Since examples are often more convincing than general reasoning, let us consider the details of the proposed approach using examples of constructing specific computer tools for preventive diagnostics.

Intelligent electrocardiograph FASEGRAF®

Coronary artery disease (CAD) remains the most common cardiac disease, which often leads to death and disability. Data from recent epidemiological studies indicate an increased occurrence of heart failure caused by coronary artery disease [12].

One of the subjective features of CAD is chest pain caused by the inadequacy of the coronary blood flow to the oxygen needs of the heart muscle. However, even

with an in-depth survey, it is not always possible to identify attacks of angina pectoris in a significant number of patients with coronary artery disease, or such attacks are atypical.

It is obvious that during mass preventive examinations it is impossible to use the method of coronary angiography for the diagnosis of CAD. Although the method is recognized as the «gold standard» in the detection of vascular stenosis and the diagnosis of coronary artery disease, coronary angiography is rather expensive and, primarily, an unsafe examination method.

A common non-invasive method for monitoring the state of the heart is based on the analysis of an electrocardiogram (ECG). However, it is known [12] that resting ECG, assessed according to generally accepted criteria, remains normal in half of patients with chronic coronary artery disease.

Therefore, the development of safe and reliable methods for diagnosing coronary heart disease in the early stages is an important problem, the solution of which can contribute to timely prescribed treatment and reduced mortality.

In the International Research and Training Center for Information Technologies and Systems of the National Academy of Sciences of Ukraine and the Ministry of Education and Science of Ukraine, an innovative method has been developed, which is called fasegraphy [14]. The method is implemented in an intelligent electrocardiograph FASEGRAF®, which has a certificate of state registration and is recommended by the Ministry of Health of Ukraine for screening myocardial ischemia [15].

ECG registration from the first standard lead is carried out using a microprocessor recorder with finger electrodes (Fig. 1, *a*). The digitized signal is fed into a smartphone via the bluetooth wireless interface, which implements intelligent signal processing procedures.

These procedures made it possible to evaluate the novel diagnostic indicator $\beta_T = D_2 / D_1$ characterizing the symmetry of the real ECG repolarization fragment on the phase plane $z(t), \dot{z}(t),$ where $z(t)$ is the signal carrying information about the electrical activity of the heart, and $\dot{z}(t)$ is a rate of change of this signal (Fig. 1, *b*, *c*).

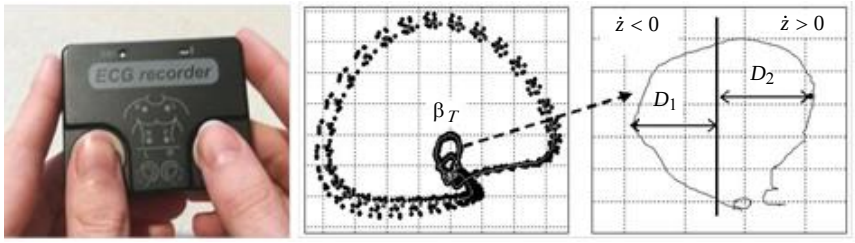

a *b* *c*

Fig. 1

Clinical studies carried out in large groups of healthy volunteers and verified patients with coronary artery disease showed that the assessment of the indicator β_T increases the sensitivity and specificity of detecting myocardial ischemia even in cases when ECG analysis in 12 traditional leads is not informative [16]. Experiments on animals carried out under artificial ischemia also confirmed the high sensitivity of the indicator β to myocardial ischemia, which was more than five times higher than the sensitivity of the traditional indicator — segment ST depression [14].

Based on these studies, the reference intervals of the indicator β_T were established:

$$\begin{aligned} &\text{Norm,} && \text{if } \beta_T < 0{,}7, \\ &\text{Satisfactory,} && \text{if } 0{,}7 \le \beta_T \le 1{,}05, \\ &\text{Attention,} && \text{if } \beta_T > 1{,}05. \end{aligned} \tag{9}$$

Using rule (9), it is possible with the help of FASEGRAPH® at home to assess the current functional state of cardiac activity and optimize the lifestyle, rationally distributing the modes of loads and rest.

Even more important information FASEGRAPH® provides on the basis of integral characteristics $x_0^{(\beta)}$ and c $\overline{S}^{(\beta)}$ calculated from the results of multiple observations in accordance with the proposed approach. The deviation $\Delta_\beta = \beta_T - x_0^{(\beta)}$ of the current result β_T from the reference result $x_0^{(\beta)}$ of a specific user allows making personalized decisions according to the scheme shown in Table 1.

Clinical studies have shown that 95 % of ECG records of healthy volunteers fall within the reference interval $\beta_T \le 0{,}87$. This makes it possible to assess the risk of developing coronary artery disease in a particular user according to the rule (8), which in this case has the form

$$\begin{aligned} &\text{Low risk of CAD, if } \beta_T \le 0{,}87, \\ &\text{Hight risk of CAD, if } \beta_T > 0{,}87. \end{aligned} \tag{10}$$

Table 1

Sign of Δ_β	Condition	Personalized solution	Message to user
+	$\lvert \Delta_\beta \rvert > 1{,}5\,\overline{S}^{(\beta)}$	Significant deterioration	Be careful!
+	$0{,}5\,\overline{S}^{(\beta)} \le \lvert \Delta_\beta \rvert \le 1{,}5\,\overline{S}^{(\beta)}$	Moderate deterioration	You need to rest
+ or –	$\lvert \Delta_\beta \rvert < 0{,}5\,\overline{S}^{(\beta)}$	Personal norm	This is your norm
–	$0{,}5\,\overline{S}^{(\beta)} \le \lvert \Delta_\beta \rvert \le 1{,}5\,\overline{S}^{(\beta)}$	Moderate improvement	You are in good shape
–	$\lvert \Delta_\beta \rvert > 1{,}5\,\overline{S}^{(\beta)}$	Significant improvement	You are in excellent shape

FASEGRAF® laid the foundation for a new direction of computer-aided preventive medicine for home use. According to the available information, a number of FASEGRAF® users who previously considered themselves healthy, with its help first learned about abnormalities in the work of the heart, which were later confirmed during in-depth medical examinations.

Intelligent RHYTHMOGRAPH on smartphone

Mathematical methods for analyzing heart variability (HRV) rate made it possible to distinguish this method as an independent non-invasive method in clinical cardiology — the method of cardiointervalography [17]. Statistical and spectral indicators of HRV reflect the work of not only the cardiovascular system, but also the mechanisms of regulation of the whole organism — the autonomic nervous system [18].

The dynamic series of cardiocycle durations (*RR*-intervals) can be estimated using a photoplethysmogram, which carries information about the blood volume of

a certain part of the body [19]. According to experts, a promising direction is the registration of a photoplethysmogram using the built-in camera of a smartphone without additional technical means [20–23].

However, on the way to the implementation of such a tempting approach, there are a number of difficulties that limit the scope of its practical application. One of the main problems arises from the «masking» of true pulse waves generated by heartbeats, and the appearance of false waves caused by random distortions and artifacts.

At the same time, our research has shown that the use of intelligent computational algorithms allows us to overcome these problems and thereby significantly reduce the probability of errors. Let us briefly consider the details of these algorithms, on the basis of which the AI-RITMOGRAPH mobile application for a smartphone has been created [24].

The user covers the smartphone camera with the phalanx of his finger, which is illuminated by a built-in flashlight (Fig. 2). A sequence of images is formed in the form of functions

$$\Psi_{\kappa m1}(x, y),\ \Psi_{\kappa m2}(x, y),\ \Psi_{\kappa m3}(x, y), \dots, \tag{11}$$

each of which characterizes the brightness of pixels with coordinates $x = k,\ y = m$ on the plane (x, y) of the image of the phalanx of the finger at fixed time instants $z = 1, 2, \dots$.

With each heartbeat, due to changes in the blood flow in the capillaries, the brightness of the video frames changes. Sequence of values

$$g_z = \frac{1}{Q_x Q_y} \sum_{k=1}^{Q_x} \sum_{m=1}^{Q_y} \Psi_{kmz}(x, y),\ \ z = 1, 2, \dots, N, \tag{12}$$

characterizing the average brightness of the images of the phalanx of the finger (Q_x, Q_x are the number of horizontally and vertically pixels) carries information about the discrete values of the pulse wave. The principle of a pulse wave recording using a smartphone camera is sown in Fig. 2.

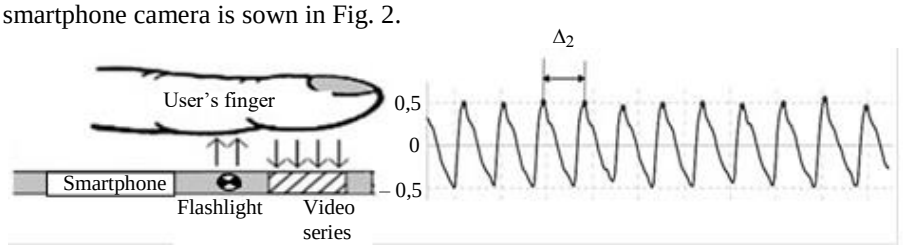

Fig. 2

The first step in processing the sequence $q_1, q_2, \dots, q_N$ is to apply a trend removal procedure that automatically adapts to the original signal. The procedure is reduced to assessing the trend using the moving average algorithm

$$G_z = \frac{1}{2W + 1} \sum_{j=-W}^{W} q[z - j]\ \ z \in [W, N - W] \tag{13}$$

with subsequent modification

$$\tilde{q}_z = q_z - G_z + \Delta, \tag{14}$$

where $W = \text{const}$ is the smoothing window, and

$$\Delta = \frac{\max\limits_{W \le z \le N-W} q_z \; - \min\limits_{W \le z \le N-W} q_z}{2}. \qquad (15)$$

The next stage of signal processing is to determine the local maxima of the pulse wave against the background of possible distortions. The use of a special adaptive procedure with a given threshold of insensitivity allows one to determine the characteristic points of the pulse wave, which divide each cycle into anacrotic and dicrotic phases (Fig. 2) and to construct an initial dynamic series of cardiointervals Δ_n, $n = 1, 2, \ldots, M$.

To increase the reliability and accuracy of determining HRV indices in the AI-RITHMOGRAPH, an original algorithm has been implemented that allows, in the process of recording a pulse wave, to automatically correct the initial dynamic series of cardiointervals Δ_1, Δ_2, … , Δ_M to remove single artifacts.

For this in the sliding window each five values of the initial dynamic series of cardiointervals are sequentially accumulated, and ranked in ascending order/. The current value of the modified array is estimated as the arithmetic average between the second, third and fourth ranked values, i.e.

$$\delta_j = \frac{d_{j-1} + d_j + d_{j+1}}{3}, \quad j = 3, \ldots, M-2. \qquad (16)$$

Since the first and last values of the current five values do not participate in procedure (16), single outliers are automatically removed. The considered procedure combines the advantages of median filtering and moving average.

AI-RITHMOGRAPH provides test results in the form of graphic images adopted in traditional cardiointervalography — scatterogram 1, histogram 2, spectrogram 3, rithmogram 4 and diagram 5 of sympatho-vagal balance, which provide visual information about the nature of the heart rhythm and it's disturbances (Fig. 3–5).

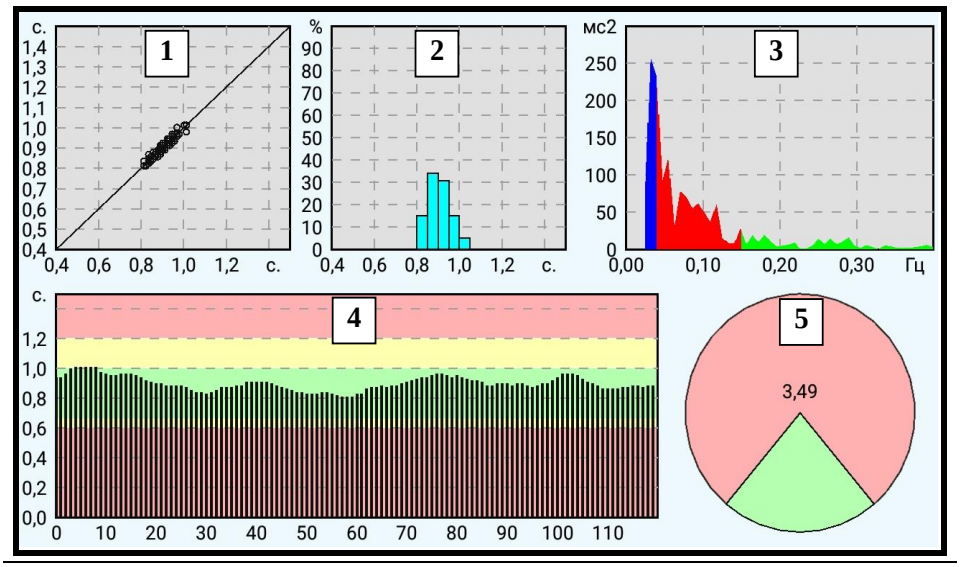

Fig. 3

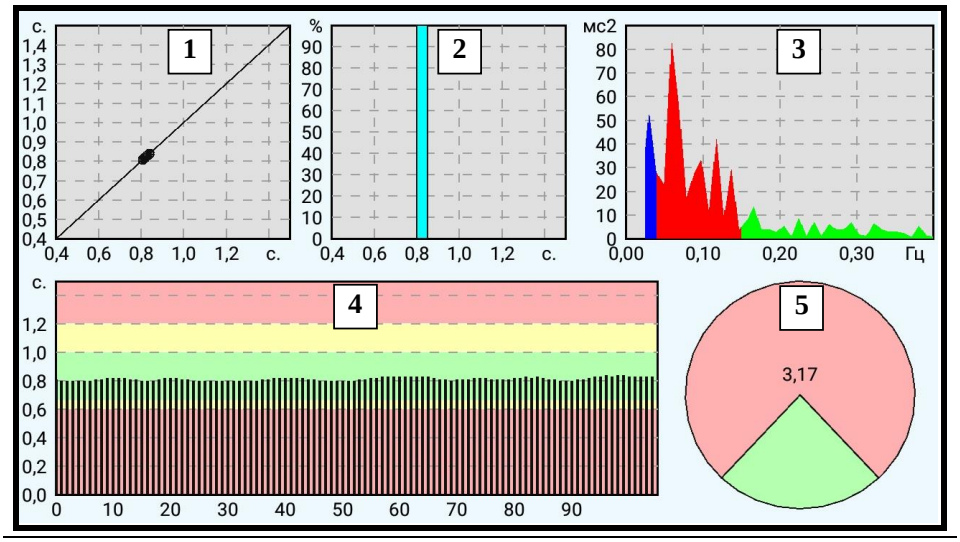

Fig. 4

In addition, AI-RITHMOGRAPH automatically calculates the values of 12 HRV indicators, including heart rate (beats / min), *SDNN* (ms), *RMSSD* (ms), *pNN*50 (%), Baevsky index, *AMo* (%), *CV* (%), *LF* / *HF* and a number of other generally accepted indicators .

Since, according to [25], until now there are no established reference values of all HRV indicators, especially with short-term recordings, the patient is provided only with information on two main indicators for self-assessment of the results (Tables 2 and 3). The rest of the indicators are accumulated in the AI-RITMOGRAPH database and can be provided to a doctor for qualified consultations. The Fig. 3 shows normal rhythm of the heart-beat. In Fig. 4 rigid rhythm is shown and arrhythmia in Fig. 5.

Table 2

Condition	Diagnosis	Indicator color
HR < 50	Bradycardia	Red
50 <= HR < 60	Bradycardia (moderate)	Yellow
60 <= HR < = 90	Normocardia	Green
90 < HR <= 100	Tachycardia (moderate)	Yellow
HR > 100	Tachycardia	Red

Table 3

Condition	Diagnosis	Indicator color
SDNN < 30	Reduced variability	Red
30 <= *SDNN* < 50	Reduced variability (moderate)	Yellow
50 <= *SDNN* < =70	Normotonia	Green
70 <= *SDNN* < =90	Variability increased (moderate)	Yellow
SDNN > 90	Variability increased	Red

In accordance with the proposed approach, AI-RITHMOGRAPH forms personified solutions according to the rules (7), (8) based on the calculation of integral characteristics x_0 and $\bar{S}$ for all HRV indicators. This allows predicting the risk of possible heart rhythm disturbances.

ISSN 1028-0979

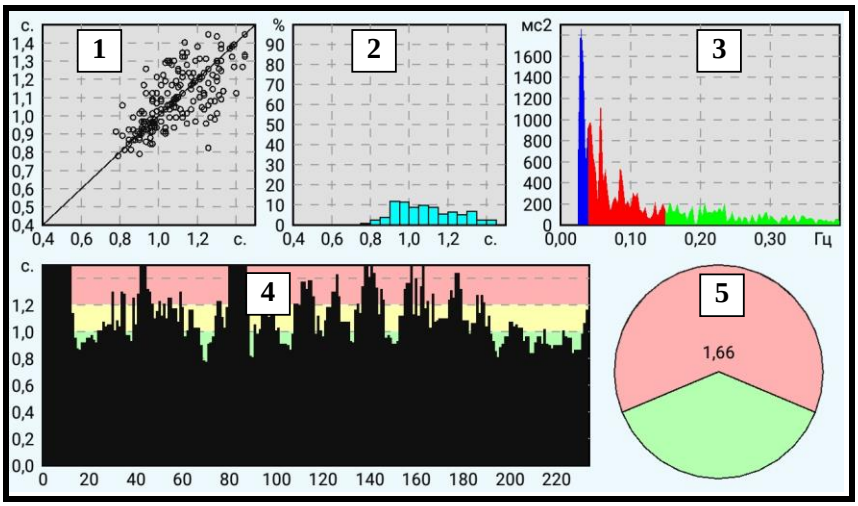

Fig. 5

AI-RITHMOGRAPH is a convenient and reliable preventive medicine tool that allows the user to receive important information about the current state of the sympathetic and parasympathetic nodes of the autonomic nervous system and predict the adaptive capabilities of organism for based on the analysis of statistical and spectral indicators of HRV.

Intelligent ARTERIOGRAPH on a smartphone

It is known that the determination of the properties of blood vessels is an important link for the early detection, prevention and treatment of diseases of the cardiovascular system. Elastic vessels allow maintaining the stroke volume of blood, reducing the load on the heart and ensuring smooth movement of blood from vessels of large diameter to vessels of smaller diameter. As a result, the pulsating blood flow from the heart is converted into a continuous and even flow through the entire vascular bed, which is very important for the normal functioning of the organism.

Aging of the organism is accompanied by a loss of elasticity of blood vessels [26]. An increase in arterial stiffness leads to an increase in the speed of propagation of the pulse wave, and this factor is currently recognized as one of the main risk factors for hypertension and the onset of coronary heart disease [27–30]. In recent years, non-invasive methods of arteriography have become widespread, providing the determination of the speed of propagation of the pulse wave in medical institutions using special equipment [31, 32].

Based on the further development of intelligent algorithms for processing finger photoplethysmogram, it was possible to create a convenient tool (AI-ARTERIOGRAPH), which allows integral assessment of the properties of blood vessels at home. The main result of this development is reliable computational algorithms focused on a smartphone, which make it possible to construct a «reference» pulse wave and detect characteristic points on it corresponding to the moment of appearance of a forward wave generated by a heart beat (point A) and a reverse pulse wave (point B) reflected from the limbs (Fig. 6).

To build a reference pulse wave, automatic selection and removal of unreliable photoplethysmogram cycles is carried out, followed by averaging only reliable cycles. The proposed approach to cycle selection differs from traditional approaches to solving the classification problem. This algorithm has a certain «intellect», which allows, in the course of processing, to form descriptions of «reliable» and «unreliable» cycles of the current photoplethysmogram. Construction of the average pulse wave is shown in Fig. 6.

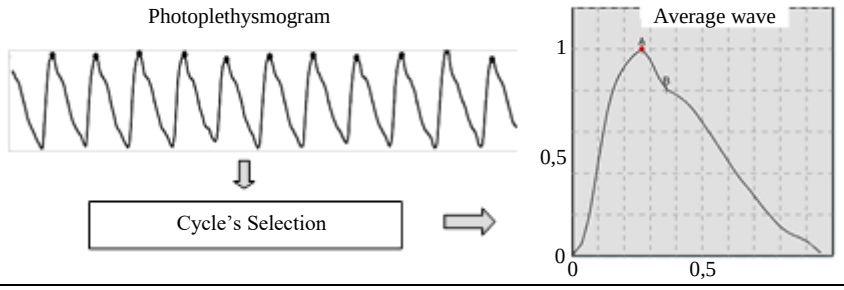

Fig. 6

The algorithm is based on a single assumption: the number $N_0^{(B)}$ of atypical cycles is significantly less than the total number N_0 of photoplethysmogram cycles (otherwise, the definition of «atypical» cycle loses meaning). This assumption made it possible to construct a procedure for isolating the most characteristic (dominant) cycle ω_0 of the recorded photoplethysmogram, using the relation

$$\omega_0 = \arg\min_{1\le\nu\le N_0} \sum_{\mu=1}^{N_0} L_{\mu\nu}, \tag{17}$$

in which $L_{\mu\nu}$ is the distance between the μ-th $(\mu = 1,..., N_0)$ and *v*-th $(\nu = 1,..., N_0)$ cycles.

To simplify the calculation of distances $L_{\mu\nu}$, the procedure for modifying fragments $\omega_n^{(i)}$ of the anacrotic $(i = I_1)$ and dicrotic $(i = I_2)$ phases of each *n*-th cycle of the processed photoplethysmogram was implemented based on the operator transformation

$$\tilde{\omega}_n^{(i)} = a_n^{(i)}\omega_n^{(i)}\left(\frac{\theta}{b_n^{(i)}}\right),\ n = 1, 2,...,\ i \in \{I_1, I_2\}, \tag{18}$$

where $a_n^{(i)}$, $b_n^{(i)}$ — parameters of linear tension (compression) in amplitude and time θ.

Since the dominant cycle ω_0 found according to (17) can be considered typical when the condition $N_B << N_0$ is satisfied the automatic classification of typical and atypical cycles can be carried out according to ordered distances

$$\Re = L(\omega_0, \omega_\lambda),\ \lambda = 1,..., N_0 - 1 \tag{19}$$

between ω_0 and the rest $N-1$ cycles of the processed photoplethysmogram.

Automatic selection of the point B on the averaged pulse wave also required the use of non-trivial algorithms based on the analysis of the first and second derivatives of the signal. Despite the fact that the procedure for numerical differentiation belongs to the number of incorrectly posed mathematical problems, the original filtering and regularization procedures made it possible to obtain acceptable estimates of the derivatives of real pulse waves and to ensure reliable detection of the point B even in cases when visual detection of this point is difficult (Fig. 7).

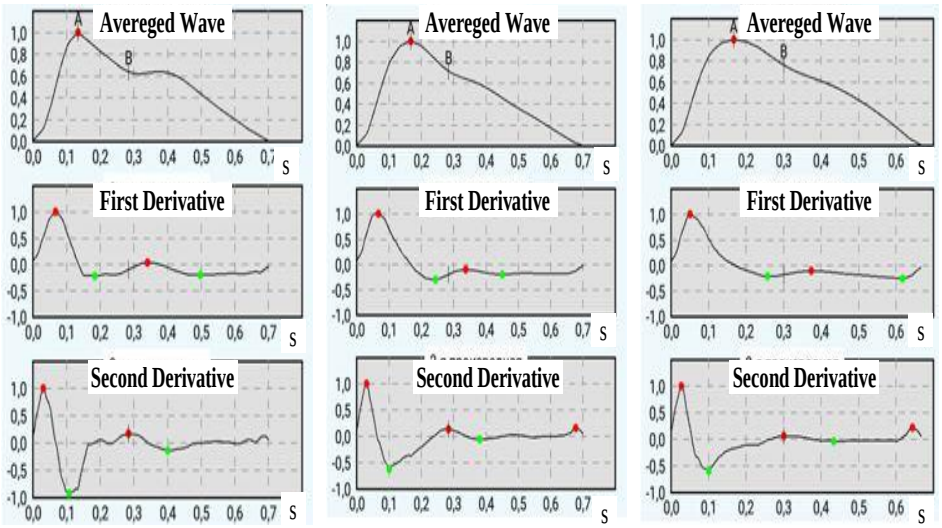

Fig. 7

Based on the averaged pulse wave, five indicators are calculated that carry diagnostic value:

$$DT = TB - TA \tag{20}$$

— the time interval between points B and A (time of pulse wave propagation, s);

$$\Delta A = \frac{AB}{AA} \tag{21}$$

— the ratio of signal amplitudes at points B and A;

$$\Delta T = \frac{DT}{T} \tag{22}$$

— the relative time of propagation of the pulse wave;

$$S = \frac{AA - AB}{DT} \tag{23}$$

— the slope of the decay of the pulse wave;

$$V = \frac{L}{DT} \tag{24}$$

— the speed of propagation of the pulse wave (m/s), where T is the total duration of the averaged pulse wave, and L is the length of the path along which the pulse wave travels over time DT. The value L is calculated from the height of the user according to a ratio derived from the standard proportions of the human body.

Having accumulated a sufficient number of observations and calculating the integral characteristics x_0 and $\bar{S}$ by indicators (20)–(24), one can make personalized decisions. In particular, according to the value $x_0^{(V)}$ characterizing the average values of the pulse wave propagation velocity V, the patient can assess the state of the blood vessels based on comparison $x_0^{(V)}$ with the reference ranges corresponding to his age.

Statistical data processing (more than 1000 photoplethysmograms of 30 volunteers of both sexes 20 to 80 years aged) confirmed that the pulse wave propaga-

tion velocity V (m/s), calculated according to (24), and person's age H (years) with a correlation coefficient $r = 0,8$ describes by linear regression equation

$$V = 5,1807 + 0,0671H, \tag{25}$$

which is consistent with the results of medical research [31, 32].

Intelligent home tonometer

Arterial hypertension is one of the most common diseases of the cardiovascular system, which affects 30 % of the adult population, and with age, the prevalence of the disease increases and reaches 65 % in people over 65 years of age [33]. If diagnosis and treatment are delayed, the disease can cause serious complications — myocardial infarction and cerebral stroke, which often result in death or disability of the patient.

Digital blood pressure monitors are one of the first digital medicine products for home use. At the first stage of the market formation, physicians expressed their concerns about the possible negative consequences of the use of these products. But by now, home blood pressure monitors are used in almost every family.

Such tonometers implement an oscillometric measurement method based on the registration of the amplitude of air pressure pulsations at the moment when the blood passes through the section of the artery compressed by the cuff. The method makes it possible to measure automatically blood pressure with weak Korotkov tones, in the presence of the phenomenon of «ascultative failure» and other effects that present difficulties in the process of automating the measurement by the Korotkov method.

Most of the home digital blood pressure monitors existing on the market, including blood pressure monitors from well-known companies Omron and Citizen (Japan), Mocrolife (Sweden), Medisana (Germany), Gamma (England) and a number of other companies, provide the user with the values of three indicators: systolic blood pressure (SBP), diastolic blood pressure (DBP), pulse rate (HR) and can store these indicators in internal memory.

At the same time, in our opinion, the intellectual potential of existing home blood pressure monitors on the market is far from being exhausted. The rapid development of microelectronics and intelligent methods of signal processing allow today to implement a number of important additional functions in home blood pressure monitors. One of these functions is the assessment of blood pressure variability [34].

We will consider the values of systolic blood pressure SBP_n, $n = 1, 2,\ldots$, which were observed in a particular user for a sufficiently long period of time (weeks, months, years), as realizations of a random variable P with a probability distribution $\Re_{SBP}$.

We denote the support of this distribution by the set

$$\Omega_{SBP} = \{P : \Re_{SBP} > 0\}, \tag{26}$$

and M_{SBP} the mean of values of SBP_n, $n = 1, 2,\ldots$.

Let further $\Omega^{(0)}_{SBP} = [100, 140]$ mmHg be the reference range of normal values SBP[2] accepted in medical practice[1]. Let us consider four options for the relative position of the sets Ω_{SBP} and $\Omega^{(0)}_{SBP}$ relative to the axis of values P (Fig. 8).

[1] To simplify the reasoning, we will not distinguish between the ranges of the norm of different age and gender groups.

Option 1. $\Omega_{SBP} \subset \Omega_{SBP}^{(0)}$, i.e. the range Ω_{SBP} of measured values is completely within the range $\Omega_{SBP}^{(0)}$ of normal values of systolic blood pressure.

Option 2. $(\Omega_{SBP} \cap \Omega_{SBP}^{(0)}) \neq \varnothing$, $\Omega_{SBP} / (\Omega_{SBP} \cap \Omega_{SBP}^{(0)}) \neq \varnothing$, i.e. the region Ω_{SBP} is only partly included in the region $\Omega_{SBP}^{(0)}$, but $M_{SBP} \in \Omega_{SBP}^{(0)}$, i.e. the average of the measured values belongs to the area of normal values of systolic blood pressure.

Option 3. $(\Omega_{SBP} \cap \Omega_{SBP}^{(0)}) \neq \varnothing$, $\Omega_{SBP} / (\Omega_{SBP} \cap \Omega_{SBP}^{(0)}) \neq \varnothing$, i.e. Ω_{SBP} is also partly included in the area $\Omega_{SBP}^{(0)}$, however $M_{SBP} \notin \Omega_{SBP}^{(0)}$, i.e. the average of the measured values does not belong to the area of normal values of systolic blood pressure.

Option 4. $(\Omega_{SBP} \cap \Omega_{SBP}^{(0)}) = \varnothing$, i.e. the range of measured values Ω_{SBP} is outside the reference range of normal values of systolic blood pressure.

In the first situation, the patient should be considered healthy. In the second situation, the results of individual measurements did not correspond to the area $\Omega_{SBP}^{(0)}$ of normal values. But since the average M_{SBP} of the measured values belongs to the region $\Omega_{SBP}^{(0)}$, such a patient can be classified as conditionally healthy with a tendency to hypertension. In the third situation, and especially in the fourth, there is nothing else but to attribute the patient to a group of patients with different degrees of arterial hypertension.

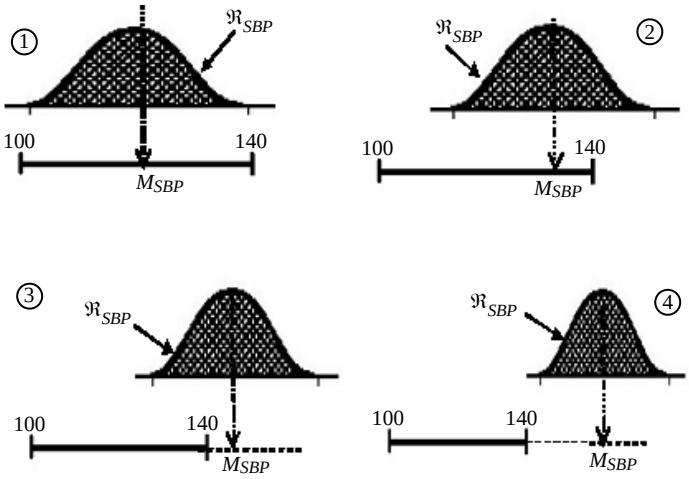

Fig. 8

Note that for the practical implementation of the proposed approach, it is not at all necessary to process the entire array of measured values SBP. It is enough for each next measurement SBP_n, $n = 1, 2, \ldots$, to correct the minimum $SBP_{\min}$ and maximum $SBP_{\max}$ obtained results according to the scheme

$$SBP_{\min,n} = SPP_n, \text{ if } SPP_n < SBP_{\min,n-1}, \tag{27}$$

$$SBP_{\max,n} = SPP_n, \text{ if } SPP_n > SBP_{\max,n-1} \tag{28}$$

and refine the current average value M_{SBP} using the recurrent formula (6), which in this case has the form

$$M_{SBP,n} = M_{SBP,n-1} + \frac{1}{n}(SBP_n - M_{SBP,n-1}), \tag{29}$$

specifying the initial conditions $M_{SBP,0} = 0$ and $SBP_{\min,0} = SBP_{\max,0} = SBP_0$.

Similarly, you can overestimate the current value of the standard deviation σ_{SBP} of systolic arterial pressure for the training sample of a particular patient.

With each measurement, we may also calculate the current values of the Pearson variation coefficient

$$V_{SBP} = \frac{\sigma_{SBM}}{M_{SBM}} \cdot 100\% \tag{30}$$

and the index

$$I_{SBP} = \frac{N_{SBP}^{(E)}}{N} \cdot 100\%, \tag{31}$$

characterizing the ratio of the number of measurements $N_{SBP}^{(E)}$ for which the systolic arterial pressure exceeded the threshold $SBP = 140$ mmHg to the total number of measurements.

In accordance with the proposed approach, for each current measurement, we will estimate the value

$$\Delta_{SBP,n} = SBP_n - M_{SBP}, \quad n = 1, 2, \ldots, \tag{32}$$

characterizing the deviation of the next results SBP_n from the previously found average value M_{SBP} and compare with the current value of the standard deviation σ_{SBP}. As a result, the home tonometer can additionally display on its screen high-quality information about the current functional state of the patient in the form of understandable graphic images (emoticons).

One of the options for generating such information is presented in Table 4.

Similarly, you can calculate the values $DBP_{\min}$, $DBP_{\max}$, M_{DBP}, σ_{DBP}, V_{DBM}, I_{DBM} allowing you to assess the long-term variability of diastolic arterial pressure, DBP_n, $n = 1, 2, \ldots$

To prevent possible distortions of integral characteristics (27)–(31), it is advisable to provide an additional button in the tonometer, with which the user can block the recalculation of these characteristics at the slightest suspicion of the erroneousness of the next measurement result due to random artifacts.

Thus, minor improvements to the home tonometer ensure the implementation of the proposed approach to personalized diagnostics and make it possible to assess the long-term variability of arterial pressure (BP) between doctor visits (visit-to-visit variability).

Table 4

Sign Δ_{SBP}	Condition	Text message	Emoticon
+	$\Delta_{SBP} > 1{,}5\sigma_{SBP}$	Dangerous condition!	
+	$0{,}5\sigma_{SBP} \le \Delta_{SBP} \le 1{,}5\sigma_{SBP}$	Be careful!	
+ or -	$\lvert\Delta_{SBP}\rvert < 0{,}5\sigma_{SBP}$	Stable condition!	
–	$0{,}5\sigma_{SBP} \le \Delta_{SBP} \le 1{,}5\sigma_{SBP}$	The condition is improving	
–	$\Delta_{SBP} > 1{,}5\sigma_{SBP}$	You are in good condition	

A qualitative assessment of the results of measuring blood pressure, realized in a household tonometer, helps the user to distribute reasonably the mode of loads and rest and determine the need for additional intake of medications prescribed by a doctor. Automatic assessment of individual characteristics (27)–(31) allows the doctor to provide more complete information about the patient for making diagnostic decisions.

Intelligent stethoscope on smartphone for detecting respiratory disorders

Acute respiratory diseases are among the most widespread and socially significant diseases that the population is facing more and more often [35]. The massive nature of these diseases presupposes a distributed system of health care delivery, when home supervision and treatment becomes important.

This task is of particular relevance in connection with the COVID-19 pandemic, since, on the one hand, it is important to diagnose timely and begin treatment of a patient with a threat of viral pneumonia, i.e. to minimize the likelihood of «missing the target», and, on the other hand, to prevent unreasonable visits to medical institutions that pose the risk of contact of a healthy patient with possible carriers of coronavirus infection, i.e. minimize the likelihood of a «false alarm».

Let us give brief information about intelligent IT [36], which allows signaling at home about possible respiratory disorders of the user and the need to visit a doctor for a more complete examination.

With the help of a microphone built into a smartphone, the patient independently registers and accumulates a training sample of respiratory noises at a certain point in the chest with a normal functional state of the respiratory organs (Fig. 9).

Using the Short-Time Fourier Transformation algorithm by sound files, phonospirogram's series $\Psi_1, \ldots, \Psi_N$ are built. Each phonospirogram is a function

$$\Psi = \Psi(f, t), \tag{33}$$

where Ψ is the energy (level) of the sound signal with the frequency $f \in F$ at the moment of time. $t \in T$. Here $F = [f_1, f_2]$ is the range of recorded frequencies in a given observation interval $T = [t_1, t_2]$.

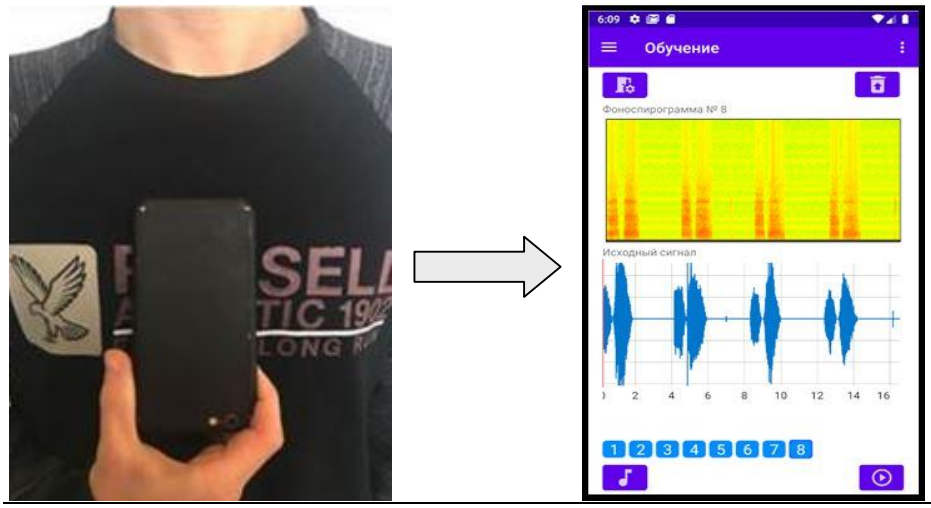

Fig. 9

The finite number of phonospirograms $\Psi_1, \ldots, \Psi_N$ represent a training sample of observations of a particular patient's respiration in a normal functional state. The proximity of two phonospirograms from the training sample is estimated by the value

$$L_{ij} = \min_{\rho=0,\ldots,\Theta} \frac{1}{K} \sum_{k=1}^{K} \left| \Psi_{\mu}^{(k)}(f, t) - \Psi_{\nu}^{(k)}(f, t-\rho) \right|, \tag{34}$$

which characterizes the average difference in sound energy $\forall k \in F \times T$, where Θ is the maximum permissible time shift of phonospirogram's characteristic points.

Next, a matrix of paired distances $L_{\mu\nu}$ between the μ-th $(\mu = 1,\ldots, N)$ and *ν*-th $(\nu = 1,\ldots, N)$ phonospirograms Ψ_{μ} and Ψ_{ν} from the training sample is formed, according to which individual integral characteristics are determined — the reference phonospirogram x_0 and the average distance $\bar{S}$ between the phonospirograms of training sample of a particular patient.

In accordance with the proposed approach, in this case, personalized decisions are made according to the scheme

$$\begin{aligned} &\text{Personal norm,} && \text{if } S(x_t, x_0) \le \lambda \bar{S}, \\ &\text{Signs of respiratiry disorder,} && \text{if } S(x_t, x_0) > \lambda \bar{S}, \end{aligned} \tag{35}$$

where x_t is the current phonospirogram, and $\lambda \ge 1$ is the coefficient characterizing the permissible deviation of the current phonospirogram from the reference one.

Of course, rule (35) does not allow classifying the type of detected respiratory disorder, but only provides the patient with important information about the advisability of contacting a medical institution to receive qualified medical care.

Conclusion

The article shows that computer tools for preventive medicine can be built on the basis of a universal approach, which involves the assessment of the physiological indicators of a specific user at home and the determination of two integral

characteristics from the accumulated results: the reference result, which is closest to all other observations from the training sample and the value characterizing the mean deviation of the results.

Such information makes it possible to increase the reliability of the decisions made about the current state of the patient and the risk of possible development of pathology, since the proposed diagnostic rules are based on the individual characteristics of the organism of a particular patient.

On the basis of the proposed approach, original preventive medicine products for home use have been developed:

- intelligent electrocardiograph FASEGRAPH;
- AI-RITHMOGRAPH for determination of statistical and spectral indicators of heart rate variability by photoplethysmogram recorded using the built-in camera of a smartphone;
- AI-ARTERIOGRAPH for integral assessment of the properties of blood vessels, including the velocity of propagation of a pulse wave, which characterizes the rigidity of arterial vessels;
- an intelligent blood pressure monitor that allows at home to assess the long-term variability of blood pressure between visits to the doctor (visit-to-visit variability);
- an intelligent stethoscope on a smartphone to detect respiratory disorders and signal on consistency of undergoing a medical examination to clarify the diagnosis.

Further research will be aimed at developing the proposed approach for the creation of similar computer tools for preventive medicine for home use, including tools that provide an assessment of visual acuity and hearing, control of the vestibular apparatus, essential tremor and other.

Л.С. Файнзільберг

УЗАГАЛЬНЕНИЙ ПІДХІД ДО ПОБУДОВИ КОМП'ЮТЕРНИХ ЗАСОБІВ ПРЕВЕНТИВНОЇ МЕДИЦИНИ ДЛЯ ДОМАШНЬОГО ЗАСТОСУВАННЯ

Для раннього виявлення та своєчасної корекції дисбалансів в організмі, які можуть викликати різні захворювання та їх ускладнення, потрібні персоніфіковані прилади, за допомогою яких можна в домашніх умовах контролювати поточний стан організму. Мета статті — розробити універсальний підхід до побудови персоніфікованих засобів превентивної медицини та на прикладах розв'язування актуальних задач продемонструвати його ефективність. Відмінна особливість запропонованого підходу полягає в тому, що користувач у домашніх умовах має можливість формувати навчальну вибірку спостережень своїх фізіологічних показників, за якою автоматично обчислюються дві інтегральні характеристики: еталонний результат, найбільш близький до решти спостережень, та величина, що характеризує середнє відхилення результатів. Побудовані персоніфіковані діагностичні правила, що забезпечують підвищення достовірності рішень про поточний функціональний стан користувача та оцінювання ризику розвитку патології. Запропоновані правила покладені в основу оригінальних засобів превентивної медицини для домашнього застосування, зокрема, інтелектуального електрокардіографа ФАЗАГРАФ® для діагностики ішемії міокарда на ранніх стадіях; програмних додатків AI-РИТМОГРАФ (для визначення показників варіабельності серцевого ритму) та AI-АРТЕРІОГРАФ (для оцінювання властивостей кровоносних судин); інтелектуального тонометра, що дозволяє оцінювати довгострокову варіабельність артеріального тиску між відвідуваннями лікаря; та інтелектуального стетоскопа для виявлення респіраторних порушень у домашніх умовах. Подальший розвиток запропонованого підходу сприятиме створенню персоніфікованих засобів для оцінки в домашніх умовах гостроти зору та слуху, контролю вестибулярного апарата, есенціального тремору та інших засобів.

L.S. Fainzilberg

GENERALIZED APPROACH TO BUILDING COMPUTER'S TOOLS OF PREVENTIVE MEDICINE FOR HOME USING

For early detection and timely correction of imbalances in the body that can lead to the development of various diseases, personalized devices are needed with which one can control the current state of the body at home. The purpose of the article is to develop a universal approach to the construction of such tools and, using examples of solving urgent problems, to demonstrate its effectiveness. A distinctive feature of the proposed approach is that the user at home has the ability to form a training sample of observations of his physiological indicators, according to which two integral characteristics are automatically calculated: the reference result, which is closest to all other observations, and the value, characterizing the average deviation of the results. Personalized diagnostic rules are proposed that ensure an increase in the reliability of decisions about the current functional state of the user and an assessment of the risk of a possible development of pathology. The proposed rules form the basis of original preventive medicine for home use, including the intelligent PHASEGRAPH® electrocardiograph for diagnosing myocardial ischemia at early stages, AI-RHYTHMOGRAPH software applications for determining heart rate variability parameters and AI-ARTERIOGRAPH for integral assessment of properties blood vessels, an intelligent blood pressure monitor that measures the long-term variability in blood pressure between doctor visits, and an intelligent stethoscope for detecting respiratory distress at home. Further development of the proposed approach will make it possible to create personalized means of assessing visual acuity and hearing acuity at home, control of the vestibular apparatus, essential tremor and other means.

1. Ambulatory cardiac monitoring: avoiding maturity through technological advancement. *Market Engineering Research. Frost & Sullivan*. Meriland. 2008. **9**. P. 325.
2. Gritsenko V.I., Fainzilberg L.S. Intelligent information technologies in digital medicine on the example of phasegraphy. Kiev : Naukova dumka, 2019. 423 p. (In Russian)
3. Litvinov A.V. Norm in medical practice: a reference guide. M .: Medpress, 2001. 144 p. (In Russian).
4. Davis C.Q., Hamilton R. Reference ranges for clinical electrophysiology of vision. *Doc Ophtalmal.* 2021. N. 143. P. 155–170. https:// doi.org/10.1007/s10633-021-09831-1.
5. Stolarz-Skrzypek K., Thijs L., Richart T. Blood pressure variability in relation to outcome in the international database of ambulatory blood pressure in relation to cardiovascular outcome. *Hypertension Research.* 2010. N 33. P. 757–766. https://doi.org/10.1038/hr.2010.110.
6. Malik M., Camm A.J. Components of heart rate variability. What they really mean and what we really measure. *American Journal of Cardiology.* 1993. **72**. P. 821–822.
7. Schijvenaars B.J.A, Van Herpen G., Kors J.A. Intraindividual variability in electrocardiograms. *Journal of Electrocardiology.* 2008. **41**, N 3. P. 190–196. https://doi.org/10.1016/j.jelectrocard.2008.01.012.
8. Swenne C.F. Neurocardiological basis for intraindividual ECG variability. *Journal of Cardiology*. 2002. N 35. P. 239–242. https://doi.org/10.1054/jelc.2002.37186.
9. Tezak Z., Kondratovich M.V., Mansfield E. US FDA and personalized medicine: in vitro diagnostic regulatory perspective. *Journal of Personalized Medicine*. 2010. N 7(5). P. 517–530. https://doi.org/10.2217/pme.10.53.
10. Wolbring G., Leopatra V. Sensors: views of staff of a disability service organization. *Journal of Personalized Medicine.* 2013. N 3. P. 23–39. DOI: 10.3390/jpm3010023.
11. Bose P., Maheshwari A., Morin P. Fast approximations for sums of distances, clustering and the Fermat — Weber problem. *Computational Geometry: Theory and Applications*. 2003. **24**, N 3. P. 135–146. https://doi.org/10.1016/S0925-7721(02)00102-5.
12. Mensah G.A., Roth G.A., Fuster V. The global burden of cardiovascular diseases and risk factors: 2020 and Beyond. *Journal of the American College of Cardiology*. 2019. **74**, N 20. P. 2529–2532. https://doi.org/10.1016/j.jacc.2019.10.009.
13. Connolly D.C., Elveback L.R., Oxman H.A. Coronary heart disease in residents of Rochester, Minnesota: Prognostic value of the resting electrocardiogram at the time of initial diagnosis of angina pectoris. *Mayo.Clin.Proc.* 1984. **59**. P. 247–250.
14. Fainzilberg L.S. Fundamentals of fasegraphy. Kiev : Osvita Ukrainy, 2017. 264 p. (In Russian)
15. Dyachuk D.D., Gritsenko V.I., Fainzilberg L.S. etc. The use of the method of fasegraphy in the screening of coronary heart disease. *Methodical recommendations of the Ministry of Health of Ukraine* № 163.16 / 13.17. Kyiv : Ukrainian Center for Scientific Medical Information and Patent and License Work. 2017. 32 p. (In Ukrainian)

16. Dyachuk D.D., Kravchenko A.N., Fainzilberg L.S., Stanislavskaya S.S., Korchinskaya Z.A., Orihovskaya K.B., Pasko V.S., Mikhalev K.A. Screening of myocardial ischemia by the method of assessing the phase of repolarization. *Ukrainian Cardiological Journal*. 2016. N 6. C. 82–89. (In Russian)
17. Corr P.B., Yamada K.A.,Witkowski F.V. Mechanisms controlling cardiac autonomic function and their relation to arrhythmogenesis. The Heart and Cardiovascular System. 1986. N-Y : Raven Press, P. 1343–1403.
18. Heart rate variability. Standards of measurement, physiological interpretation and clinical use. *Circulation.* 1996. **93**. P. 1043–1065. https://doi.org/10.1161/01.CIR.93.5.1043
19. Saquib N., Papon M.T.I., Ahmad I., Rachman A. Measurement of heart rate using photoplethysmography. *Proceeding of 2015 International Conference on Networking Systems and Security.* Dhaka, 2015. P. 158–163. https://doi.org/10.1109/NSysS.2015.7043525.
20. Papon M.T.I., Ahmad I., Saquib N., Rahman A. Non-invasive heart rate measuring smartphone applications using on-board cameras: A short survey. *Proceeding of 2015 International Conference on Networking Systems and Security*. Dhaka, 2015. P. 1–6. https://doi.org/10.1109/NSysS.2015.7043533.
21. Laure D., Paramonov I. Improved algorithm for heart rate measurement using mobile phone camera. *Proceedings of the 13th Conference of Open Innovations Association FRUCT and 2nd Seminar on e-Tourism for Karelia and Oulu Region*. 2013. P. 8593. https://doi.org/10.23919/FRUCT.2013.8124232.
22. Boland P. The emerging role of cell phone technology in ambulatory care. *Journal of Ambulatory Care Managemen.* 2007. **30**, N 2. P. 126–133. https://doi.org/10.1097/01.JAC.0000264602.19629.84.
23. Jonathan E., Leahy M. Investigating a smartphone imaging unit for photoplethysmography. *Physiol Measurements.* 2010. **31**, N 11. P. 79–83. https://doi.org/10.1088/0967-3334/31/11/N01.
24. Fainzilberg L.S. Smart digital medicine for home use. *Clinical informatics and telemedicine.* 2020. **15**, N 16. P. 45–56. https://doi.org/10.31071/kit2020.16.03. (In Russian).
25. Tegegne B.S., Man T., van Roon A.M., Snieder H., Riese H. Reference values of heart rate variability from 10-second resting electrocardiograms: the lifelines cohort study. *European Journal of Preventive Cardiology.* 2020. **27** (19). P. 2191–2194. https://doi.org/10.1177/2047487319872567.
26. Lehmann E.D. Elastic properties of the aorta. *Lancet.* 1993. N 342. P. 1417. https://doi.org/10.1016/0140-6736(93)92772-l
27. Benetos A., Laurent S., Hoeks A.P., Boutotiyrie P.H., Safar M.E. Arterial alterations with ageing and high blood pressure. A noninvasive study of carotid and femoral arteries. *Arterioscler Thromb.* 1993. N 13. P. 90–97. https://doi.org/10.1161/01.atv.13.1.90
28. Cameron J.D., Jennings Q.L., Dart A.M. The relationship between arterial compliance, age, blood pressure and serum lipid levels. *Journal of Hypertension.* 1995. N 13. P. 1718–1723.
29. Laurent S, Boutouyrie P, Asmar R. Aortic stiffness is an independent predictor of all-cause and cardiovascular mortality in hypertensive patients. *Hypertension.* 2001. **37**, N 5. P. 1236–1241. https://doi.org/10.1161/01.hyp.37.5.1236
30. Blacher J., Asmar R., Djane S. Aortic pulse wave velocity as a marker of cardiovascular risk in hypertensive patients. *Hypertension.* 1999. **33**, N 5. P. 1111–1117. https://doi.org/10.1161/01.hyp.33.5.1111.
31. Asmar R., Benetos A. Topouchian J. Assessment of arterial distensibility by automatic pulse wave velocity measurement. Validation and clinical application studies. *Hypertension.* 1995. **26**, N 3. P. 485–490. https://doi.org/10.1161/01.HYP.26.3.485.
32. Asmar R., Topouchian J., Pannier B. Pulse wave velocity as endpoint in large-scale intervention trial. *The Complior study. Journal of Hypertension.* 2001. 19, N 4. P. 813–818. https://doi.org/10.1097/00004872-200104000-00019.
33. Dilaveris P.E. Richter D.J. Gialafos J.E. Inadequate blood pressure control in a low risk Mediterranean population. *European Heart Journal.* 1999. N 20. P. 1845. DOI: 10.1053/euhj.1999.1847.
34. Fainzilberg L.S. Expanding of intellectual possibilities of digital tonometers for home using. *Control Systems and Computers.* 2020. N 1. P. 60–70. https://doi.org/10.15407/usim.2020.01.060.
35. Hansen M.P., Bjerrum L., Gahrn-Hansen B. Quality indicators for diagnosis and treatment of respiratory tract infections in general practice: A modified Delphi study. *Scandinavian Journal of Primary Health Care.* 2010. N 28. P. 4–11. https://doi.org/10.3109/02813431003602724.
36. Fainzilberg L.S., Solovey S.R. Self-learning information technology for detecting respiratory disorders in home conditions. *Cybernetics and computer engineering.* 2021. N 2 (204). P. 64–83. https://doi.org/10.15407/kvt204.02.064.

Submited 11.01. 2022